

Article

# Processing of Oxidized Lead–Zinc Ore by Co-Roasting with Pyrite-Bearing Ore

Inna Germanovna Antropova, Pavel Anatolevich Gulyashinov , Aryuna Dugarzhapovna Budaeva, Ilya Punsukovich Dashiev  and Darya Petrovna Khomoksonova \* 

Laboratory of Chemistry and Technology of Natural Raw Materials, Baikal Institute of Nature Management, Siberian Branch of the Russian Academy of Sciences, Ulan-Ude 670047, Russia; gulpasha@mail.ru (P.A.G.); abud@binm.ru (A.D.B.); ilya.dashiev.02@mail.ru (I.P.D.)

\* Correspondence: darkh@binm.ru

**Abstract:** The world reserves of oxidized lead–zinc ores are large, but their processing faces significant difficulties due to their refractory nature. This paper presents a novel approach to the preparation of refractory oxidized lead ores for flotation. The proposed method is based on the co-roasting of oxidized lead-bearing ores from the Ozernoye polymetallic deposit (Western Transbaikalia, Russia) with fine-grained sulfide lead–zinc ore sourced from the same deposit and the addition of calcium oxide. This method allows for the activation of mineral complexes, the sulfidation of oxidized lead–zinc minerals, and the minimization of the amount of sulfur dioxide gas emitted. Co-roasting oxidized lead–zinc ore with sulfide ore (10–30 wt. pct) at 650–700 °C has been shown to result in the selective oxidation of pyrite and sulfidation of oxidized lead and zinc minerals. The proposed method of processing polymetallic ores is capable of simultaneously involving not only oxidized lead–zinc ores but also refractory sulfide ores, thereby extending the operational lifespan of the mining enterprise and reducing the environmental impact.

**Keywords:** oxidized lead–zinc ore; sulfidation roasting; sulfide ore as a sulfidation agent; sulfur dioxide absorption



**Citation:** Antropova, I.G.; Gulyashinov, P.A.; Budaeva, A.D.; Dashiev, I.P.; Khomoksonova, D.P. Processing of Oxidized Lead–Zinc Ore by Co-Roasting with Pyrite-Bearing Ore. *Minerals* **2024**, *14*, 1241. <https://doi.org/10.3390/min14121241>

Academic Editor: Frédéric J. Doucet

Received: 22 October 2024

Revised: 29 November 2024

Accepted: 3 December 2024

Published: 5 December 2024



**Copyright:** © 2024 by the authors. Licensee MDPI, Basel, Switzerland. This article is an open access article distributed under the terms and conditions of the Creative Commons Attribution (CC BY) license (<https://creativecommons.org/licenses/by/4.0/>).

## 1. Introduction

The primary global reserves of lead and zinc are found in countries such as Canada, the USA, Australia, Kazakhstan, Russia, China, India, Mexico, South Africa, and Peru. At the same time, polymetallic deposits located in Buryatia (Russia) are estimated to account for 26.1 pct of Russian lead resources and 50.9 pct of zinc resources [1–3].

The Ozernoye deposit is situated in Buryatia, although it is not within the Lake Baikal protection zone. It is the second largest zinc deposit in Russia and the eighth largest in the world. The Ozernoye deposit is characterized by favorable mining conditions, convenient geographical, economic, and environmental location. The enrichment plant at the deposit with a capacity of six million tons of ore per year is scheduled to be commissioned in 2024. The ores at the deposit are rich in lead and zinc with very low copper content: the ratio of Pb:Zn:Cu is 1:6:0.05 [4]. The estimated reserves of polymetallic ores in the deposit is approximately 157 million tons. The average grade of zinc is 6.16 pct; lead, 1.17 pct; cadmium, 0.017 pct; and silver, 35 g/ton.

The Ozernoye deposit is complex, but the main industrial value is made up by sulfide–polymetallic ores [5–9]. At the same time, sulfide ores from the Ozernoye are heterogeneous and complex by mineral and phase composition. They are characterized by an increased content of refractory ores, which contain disseminated lead, zinc, and iron minerals, in addition to a significant presence of fine intergrown crystals consisting of sulfide minerals. The main ore minerals are pyrite (FeS<sub>2</sub>) and sphalerite (ZnS), with galena (PbS) being less abundant. The host rocks at the Ozernoye deposit consist of limestones, andesite porphyrite, andesite–basalt porphyrite, and basaltic porphyrite. An oxidation zone

20–30 m thick is distributed throughout the deposit, reaching depths of 50–70 m along fault zones [1,8]. Iron hydroxides predominate in the oxidized ores, along with sulfates, oxides, and carbonates of lead and zinc. The lead content in oxidized ores varies from 0.3 pct to 20 pct, while the zinc content ranges from 0.3 pct to 1.8 pct.

During the design phase for the Ozernoye deposit, a flotation enrichment scheme for sulfide ores was planned. The reserves of oxidized ores amount to 5.788 thousand tons; however, due to the lack of rational processing technology, these ores are planned to be stored near the quarry in an open-air storage facility for oxidized ores.

It is well established that oxidized ores of heavy non-ferrous metals are typically refractory ores, which are difficult to enrich. Therefore, for the extraction of heavy non-ferrous metals from difficult-to-process ores and waste from non-ferrous metallurgy, flotation is practically impossible; thus, it is advisable to employ combined schemes involving hydro- or pyro-metallurgical operations [10–27]. For instance, a combined scheme has been proposed for the processing of refractory oxidized ore containing beudantite and plumbojarosite. The initial stage of the proposed scheme involves roasting the ore at 600–700 °C, which serves to expose the complex minerals and induce the formation of microcracks. This process also results in the decomposition of plumbojarosite, which is then leached with a sodium chloride solution. The disadvantages of this method include the combination of roasting, leaching, precipitation, etc. in a single scheme, as well as the relatively low extraction of lead in the solution (up to 85 pct). In a study conducted by the authors of [17], technology was developed for extracting valuable metals from oxidized lead–zinc ore (Yunnan Province, China) by roasting with pyrite and coal. One of the limitations of this technology is the use of pure pyrite as a sulfidation agent. In previous works [19,20], elemental sulfur was proposed as a sulfidation agent, and the possibility of thermal sulfidation of zinc oxides with sulfur in the presence of coal and iron oxides was also investigated [21]. It has been demonstrated that the sulfidation process in the presence of coal contributes to the reduction of sulfur dioxide gas formation. Furthermore, the iron sulfides formed in the studied system may also participate in the sulfidation process.

In previous studies, we developed methods for the sulfidation of ores from several lead–zinc deposits in Western Transbaikalia. These methods were based on sulfidation roasting of the ore in a water vapor atmosphere, using industrial pyrite concentrates as sulfidation agents, which significantly increased the extraction of valuable metals [28,29]. However, these methods had limitations, including a reduction in the content of valuable metals in oxidized ores (due to the use of pyrite concentrates) and the presence of residual hydrogen sulfide in the flue gases (resulting from roasting in a steam atmosphere).

To improve the environmental safety of the thermal sulfidation process and reduce processing costs, this paper proposes an improved technology for preparing refractory ores for subsequent flotation. The efficiency of this process can be enhanced by using pyrite-bearing lead–zinc ore (including refractory varieties) from the same deposit as the sulfidation agent, thereby eliminating the need for water and reducing sulfur-containing gas emissions.

In this study, for the first time, the process of sulfidation roasting the refractory oxidized lead–zinc ores (using ores from the Ozernoye deposit as an example), using fine-grained sulfide lead–zinc ore from the same deposit as the sulfidation agent, was investigated. In contrast to previous studies, this method did not require a water supply and included the addition of calcium oxide.

## 2. Materials and Methods

### 2.1. Materials

In this study we used samples of oxidized and sulfide ores from the Ozernoye polymetallic deposit. According to the XRD data (Figure 1a), the main minerals in the oxidized ore sample were goethite (FeOOH) (39.72 wt. pct), quartz (SiO<sub>2</sub>) (42.56 wt. pct), plumbojarosite (PbFe<sub>6</sub>(OH)<sub>12</sub>(SO<sub>4</sub>)<sub>4</sub>) (16.08 wt. pct), and cerussite (PbCO<sub>3</sub>) (1.49 wt. pct), as well as hetaerolite (ZnMn<sub>2</sub>O<sub>4</sub>), the mass fraction of which in the sample was about 0.15 wt. pct [30].

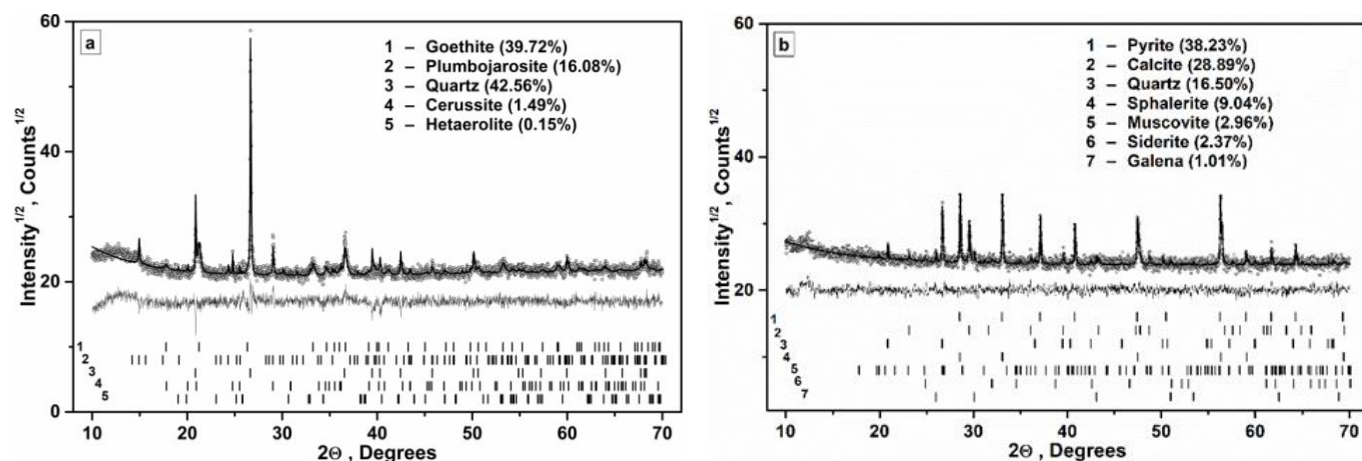


**Figure 1.** (a) Rietveld refined XRD pattern of the oxidized ore sample. (b) Rietveld refined XRD pattern of the sulfide ore sample.

The main minerals of the sulfide ore were pyrite ( $\text{FeS}_2$ ) (38.23 wt. pct), sphalerite ( $\text{ZnS}$ ) (9.04 wt. pct), and galena ( $\text{PbS}$ ) (1.01 wt. pct). Among rock-forming minerals, calcite ( $\text{CaCO}_3$ ) (28.89 wt. pct), quartz ( $\text{SiO}_2$ ) (16.50 wt. pct), small amounts of siderite ( $\text{FeCO}_3$ ) (2.37 wt. pct) and muscovite ( $\text{KAl}_2(\text{AlSi}_3\text{O}_{10})(\text{OH})_2$ ) (2.96 wt. pct) were found (Figure 1b).

According to the chemical analysis (Table 1), the main valuable components in the oxidized ore sample were lead (4.11 wt. pct) and silver (100 g/ton). The content of total iron was 29.73 pct, while the contents of zinc and manganese were low—0.04 and 0.15 pct, respectively. The silicon oxide content was 42.56 pct.

**Table 1.** The results of chemical analysis of the oxidized and sulfide ores.

Sample	Component, wt. %								
	$\text{SiO}_2$	$\text{Al}_2\text{O}_3$	$\text{Fe}_{\text{total}}$	$\text{K}_2\text{O}$	$\text{CaO}$	$\text{MnO}$	Zn	Pb	Ag, g/t
Oxidized ore	42.56	0.06	29.73	0.11	0.21	0.15	0.04	4.11	100
Sulfide ore	17.97	1.15	18.97	0.36	16.74	0.08	6.07	0.87	25

The valuable components in the sulfide ore sample were Zn (6.07 pct), Pb (0.87 pct), and Ag (25 g/ton). The content of total iron in this ore sample was 18.97 pct, and the contents of silica and calcium oxide were 17.97 pct and 16.74 pct, respectively. So, the investigated ore from the Ozernoye deposit was complex and contained silver. A significant part of the world's silver reserves is associated with lead–zinc ores [31], and it can be easily separated by flotation into a galena concentrate [28].

A mineralogical study of the sulfide ore sample was carried out. It showed that the sample belonged to the sulfide ores with a layered, banded texture—this type accounts for 23 to 30 pct of the reserves in the Ozernoye deposit. Microscopic examination of the polished section revealed sericite–quartz–carbonate–sulfide rock including fragments of andesite, limestone, and granitoids (Figure 2). The rock contained ore minerals (sulfides), which were mainly pyrite and sphalerite. Individual flakes of muscovite (sericite), quartz, and carbonates, together with aggregates of quartz–sericite–carbonate composition, were found in the sulfide mass.

Ore minerals were formed by the fine-grained intergrowths of pyrite and sphalerite crystals with a mixture of galena (as part of pyrite aggregates). The pyrite grains ranged in size from 4 to 40 microns. Pyrite crystals were aggregated in clusters within sphalerite formations. Sphalerite particles of irregular isometric shape (up to 150 microns) were observed along the margins of the banded sphalerite–pyrite aggregates. Individual sphalerite grains were also found within the main non-metallic mass. Galena formed small (2–30 microns) xenomorphic formations that were visible only at high magnification (50× lens). Galenite

also occurred as rare grains up to 50–70 microns in size and were sometimes associated with sphalerite.

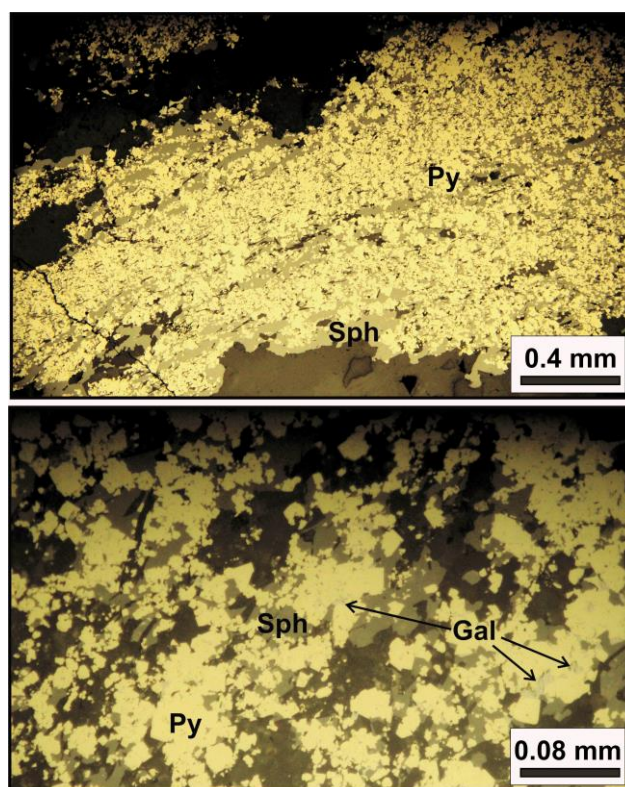


**Figure 2.** Microphotograph of a polished section of a sulfide ore sample from the Ozernoye deposit: Py—pyrite; Sph—sphalerite; Gal—galena.

Thus, the sulfide ore sample showed a significant intergrowth of sulfide crystals, small grain size (1–50 microns), and relatively simple mineralogical composition. Typically, such sulfide ores are subjected to very fine grinding (to 2–50 microns) prior to flotation, and even so, acceptable recoveries are not always achieved [32–41].

## 2.2. Methods

Experiments on the sulfidation roasting of oxidized ore were carried out in a laboratory plant of the flow type with a flue gas collection system. Pyrite-bearing lead–zinc ore was used as the sulfidation agent. A ground sample, with a mass of 1.5 g and a particle size of 0.25 mm, was placed in a heated furnace. The amount of sulfidation agent varied from 10 wt. pct to 30 wt. pct of the total mass of the sample, and the roasting time was 15 or 30 min.

The interaction of the oxidized and sulfide ores was studied by thermal analysis with subsequent analysis of the cinders by the X-ray diffraction (XRD) method. Thermal analysis for the mixture of the oxidized and sulfide forms of the lead–zinc ore was performed using the thermogravimetric differential scanning calorimetric (TG-DTA/DSC) method on a Netzsch Jupiter STA 449C Thermoanalyzer. To record thermograms, a sample was loaded into a platinum crucible under an argon atmosphere and subsequently heated to 850 °C at a rate of 10 °C/min. Phase identification was conducted using powder XRD with a Bruker D8 ADVANCE diffractometer (Cu–K $\alpha$  radiation), equipped with a VANTEC linear detector. Quantitative phase analysis and refinement of the elementary cell parameters were carried out by the Rietveld method using the TOPAS program. Mineragraphic study for the sulfide ore, used as a sulfidation agent, and the cinder was performed using an Olympus BX-51 optical microscope and a LEO-1430VP scanning electron microscope (SEM) equipped with an INCAEnergy 350 energy-dispersive microanalysis system at the N.L. Dobretsov Geological Institute SB RAS. To evaluate the thermodynamic favorability of the reactions,

the Temkin–Schwartzman method was employed [42–44]. The sulfur dioxide content of the flue gases was quantified by analyzing sludge in the absorption tanks containing chemisorption solutions.

### 3. Results and Discussion

#### 3.1. The Results of Research on the Sulphidation Roasting of Oxidized Ore

In this study, we employed sulfidation roasting of the oxidized ore at the stage of its preparation for flotation in order to adapt this process to the specific mineralogical composition of the oxidized lead–zinc ore from the Ozernoye deposit. One of its key features is the presence of the oxidized lead mineral plumbojarosite ( $\text{PbFe}_6(\text{OH})_{12}(\text{SO}_4)_4$ ) in the ore, which is poorly extractable using conventional enrichment methods.

A thermal analysis of a mixture of the oxidized and sulfide forms of the lead–zinc ore (with a sulfide form content of 30 wt. pct) was performed. The endothermic peak on the DTA curve at 280–300 °C (Figure 3a) corresponded to the transition of goethite to hematite with the release of water (mass loss was 7 pct). Another endothermic peak (520–540 °C) corresponded to the initial decomposition of plumbojarosite, accompanied by the formation of basic lead sulfate and water release. Mass losses above 400 °C were associated with the decomposition of cerussite and muscovite. The exothermic effect at 405 °C can be attributed to the interaction of pyrite decomposition products with superheated water vapor, which was accompanied by the formation of hydrogen sulfide and iron oxides. The second exothermic effect observed in the temperature range of 580–640 °C was likely associated with the formation of lead and zinc sulfides (during the interaction of sulfur-containing compounds with the decomposition products of plumbojarosite, cerussite, and hetaerolite).

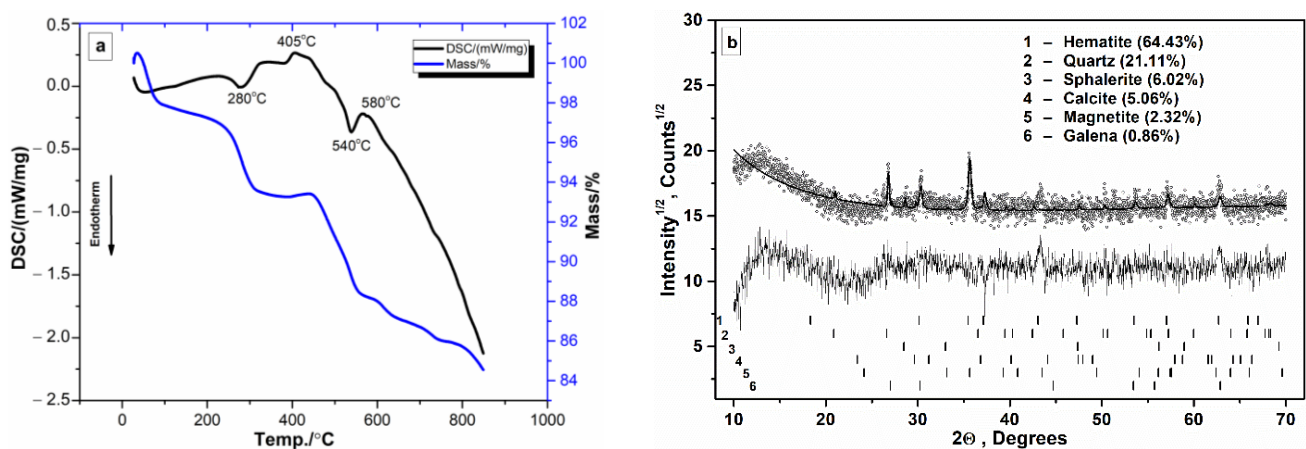


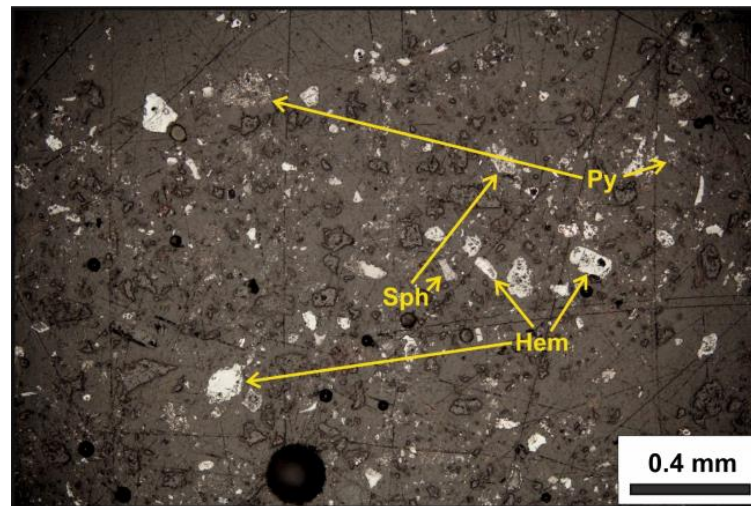
**Figure 3.** (a) TG and DSC curves for the mixture of the oxidized and sulfide forms of the lead–zinc ore. (b) XRF of the sample after the completion of thermal analysis.

XRD phase analysis (Figure 3b) revealed that the major components of the sample after heating to 850 °C were sphalerite, galena, hematite, magnetite, quartz, and calcite. No oxidized lead and zinc minerals were detected.

In order to select the optimum roasting temperature and duration, ore containing 30 wt. pct of the sulfidation component was used in the experiments. It was determined that at a temperature of 650 °C and a roasting time of 15 min, the oxidation process of pyrite was not complete (Table 2, Figure 4). Small particles of ore and non-metallic minerals up to 200 microns in diameter were found in the pyrite cinder (Figure 4). The total content of the newly formed and relict sulfide minerals was approximately 40–45 vol. pct.

**Table 2.** Reaction products detected by XRD analysis.

T, °C	Compounds Detected ( $\tau_{\text{roasting}}$ , min)	
	15	30
650	PbS, ZnS <sub>wurtz.</sub> , Fe <sub>2</sub> O <sub>3</sub> , Fe <sub>3</sub> O <sub>4</sub> , FeS <sub>2</sub> (trace), SiO <sub>2</sub> , CaCO <sub>3</sub> , CaSO <sub>4</sub>	ZnS <sub>sph.</sub> , ZnS <sub>wurtz.</sub> , PbS, Fe <sub>3</sub> O <sub>4</sub> , Fe <sub>2</sub> O <sub>3</sub> , SiO <sub>2</sub> , CaCO <sub>3</sub> , CaSO <sub>4</sub>
700	ZnS <sub>wurtz.</sub> , ZnS <sub>sph.</sub> , PbS, Fe <sub>3</sub> O <sub>4</sub> , Fe <sub>2</sub> O <sub>3</sub> , SiO <sub>2</sub> , CaCO <sub>3</sub> , CaSO <sub>4</sub>	ZnS <sub>sph.</sub> , PbS, Fe <sub>2</sub> O <sub>3</sub> , Fe <sub>3</sub> O <sub>4</sub> , SiO <sub>2</sub> , CaCO <sub>3</sub> , CaSO <sub>4</sub>

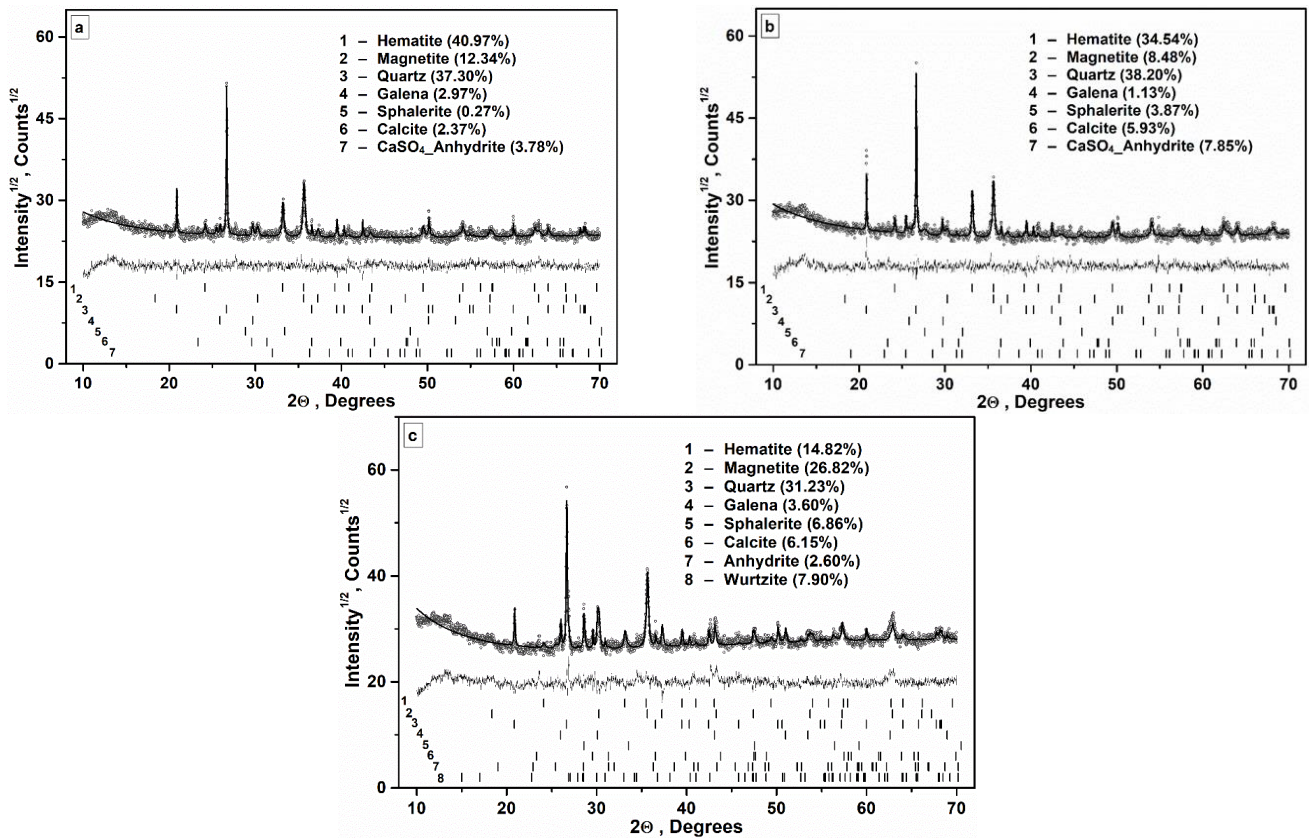
**Figure 4.** Microphotograph of the cinder after 15 min of roasting.

Hematite (Hem) was the most common ore mineral and formed relatively large angular grains with a hypidiomorphic texture. The grains were isometric in shape, sometimes nearly rounded and less often irregularly elongated. Furthermore, grains of sphalerite (Sph), with a diameter of 50–150  $\mu\text{m}$ , and skeleton crystal structures of pyrite (Py) and galena were observed. As magnetite had previously been removed from the studied preparation (nonmagnetic fraction), it occurred only as rare relicts in the central parts of the hematite grains.

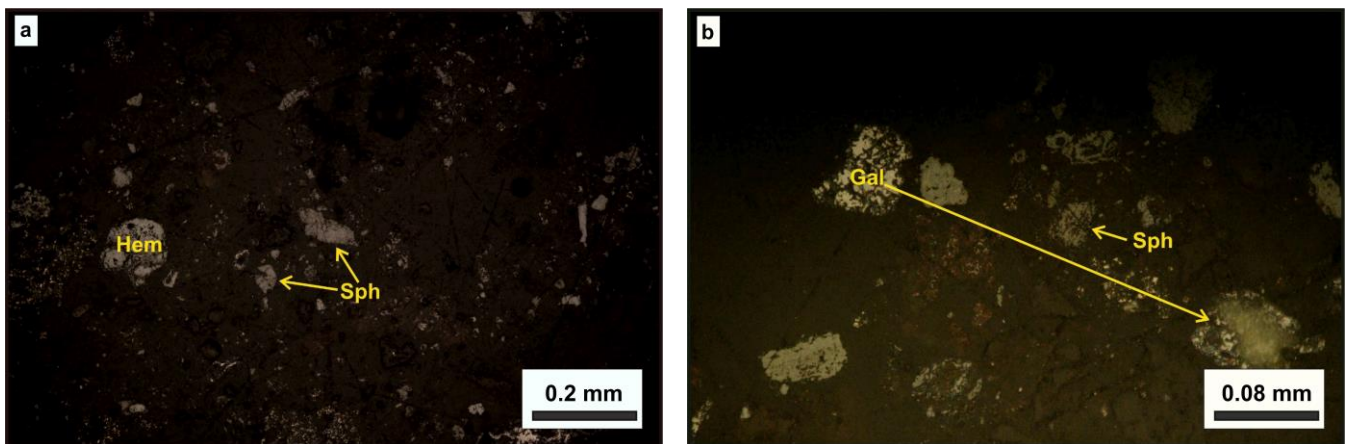
It was determined that the complete oxidation of pyrite could be achieved at 700 °C (for 15 or 30 min) or at 650 °C (for 30 min). The optimal conditions for the complete oxidation of pyrite and sulfidation of the oxidized forms of lead and zinc (at a sulfide ore content of 30 wt. pct) were found to be a temperature of 650 °C and a duration of 30 min (Figure 5c). Further studies using other (smaller) amounts of sulfide ore were carried out under the previously identified optimal conditions.

At a sulfide ore content of 10 wt. pct and a duration of 30 min, the presence of lead and zinc sulfides, as well as the iron-bearing phases of hematite and magnetite, was observed in the cinder (Figure 5a). Upon increasing the sulfide ore content to 20 wt. pct, the complete oxidation of pyrite and formation of lead and zinc sulfides were also observed (Figure 5b).

No oxidized lead and zinc minerals were detected. It was observed that calcite CaCO<sub>3</sub> reacted with sulfur dioxide emitted during the roasting process, leading to the formation of anhydrite CaSO<sub>4</sub>. According to DSC data, plumbojarosite (PbFe<sub>6</sub>(OH)<sub>12</sub>(SO<sub>4</sub>)<sub>4</sub>) decomposed at 500–600 °C to form lead sulfate and hematite, and released a crystallization of water and sulfur dioxide gas. All oxidized lead and zinc minerals were completely converted to sulfide forms under the indicated experimental conditions. It should be noted that at lower contents of the sulfidizer (10 wt. pct and 20 wt. pct), only galena and sphalerite were detected among sulfides, but wurtzite was not formed (Figure 6).

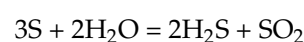


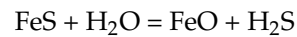
**Figure 5.** XRD of the samples of cinder with the addition of: (a) 10 wt. pct of the sulfidation agent; (b) 20 wt. pct of the sulfidation agent; (c) 30 wt. pct of the sulfidation agent.



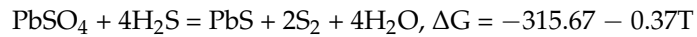
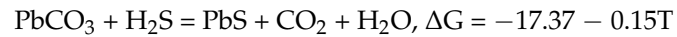
**Figure 6.** Microphotograph of the non-magnetic fraction of the cinder: (a) grains of the newly formed sphalerite (Sph) and round-shaped formations of hematite (Hem); (b) morphology of the galena (Gal) and sphalerite (Sph) formations.

The proposed mechanism involved the sulfidation of the oxidized forms of lead and zinc during the co-roasting of the oxidized ore, which contained goethite and plumbojarosite with sulfide ore. The decomposition of goethite ( $\text{FeOOH}$ ) and plumbojarosite ( $\text{PbFe}_6(\text{OH})_{12}(\text{SO}_4)_4$ ) at high temperatures produced water vapor, which reacted with elemental sulfur and iron sulfide (decomposition products of pyrite) to form hydrogen sulfide:

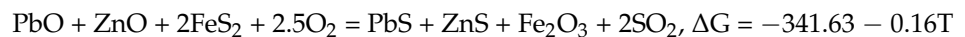
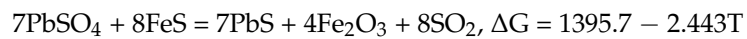
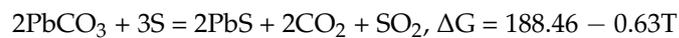




Iron oxide (FeO) was further oxidized to form iron (II) oxide (Fe<sub>2</sub>O<sub>3</sub>). Hydrogen sulfide was involved in the sulfidation of cerussite (and probably its decomposition product, PbO) and the decomposed minerals plumbojarosite and hetaerolite:



The following reactions may also occur if the amount of hydrogen sulfide in the system is insufficient:

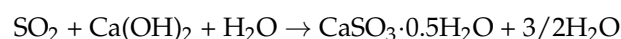


Thus, at roasting temperatures of 650–700 °C (923–973 K), the calculated values of  $\Delta G$  for all the above reactions have negative values, indicating the possibility of their occurrence.

### 3.2. The Results of Research on Reducing SO<sub>2</sub> Content in Exhaust Gases

According to the analysis data, the flue gases, generated during sulfidation, contained sulfur dioxide, but hydrogen sulfide was not detected. The formation of sulfur dioxide gas during sulfidation roasting of the oxidized zinc and lead minerals using pyrite or elemental sulfur as a sulfidation agent has been reported in a number of studies [17–21].

One of the most commonly used methods for cleaning flue gases from SO<sub>2</sub> at low concentrations is the sulfation process [45–48]. Gases containing SO<sub>2</sub> are absorbed by the Ca(OH)<sub>2</sub> suspension in a scrubber, with the formation of hemihydrate or calcium sulfite:



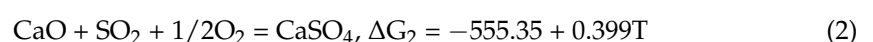
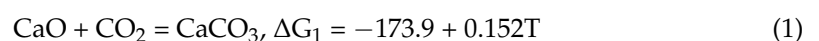
Gypsum is further formed when sulfite was oxidized by the addition of oxygen:

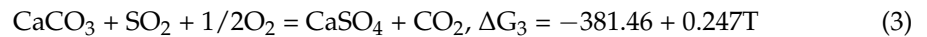


Instead of calcium hydroxide suspension, the authors [49,50] proposed the use of Ca- and Mg-containing wastes of the phosphorus production and construction industries to capture SO<sub>2</sub>. These cleaning methods have a number of advantages, such as the relative simplicity and compatibility with other processes, but they require the use of specialized equipment and its maintenance, which significantly increase the cost of the production process.

Binding SO<sub>2</sub> in the cinder by adding inexpensive reagents to the initial mixture can serve as a promising and cost-effective way to utilize flue gases in the process of the sulfidation of oxidized lead–zinc ores.

Thermodynamic analysis of the possible reactions of the gas phase components with calcium oxide and calcium carbonate at different temperatures was performed.





According to these calculations, the most efficient process was the interaction of sulfur dioxide with calcium oxide to form  $\text{CaSO}_4$ .

In order to reduce the content of  $\text{SO}_2$  in the flue gases, experiments on roasting with the addition of calcium oxide to the initial mixture were carried out. The roasting time was 30 min, the mass of the sample of the studied oxidized and sulfide ore of the Ozernoye deposit was 1.5 g, and the amount of the added additive varied from 3 to 9 wt. pct of the sample mass (0.05 g, 0.1 g, and 0.15 g). The solutions of  $\text{H}_2\text{O}_2$ ,  $\text{Na}_2\text{CO}_3$ , and a suspension of  $\text{Ca}(\text{OH})_2$  were used as the sulfur dioxide absorbers.

The data in Table 3 show that the calcium hydroxide suspension absorbed the residual sulfur dioxide most effectively, so we used it for further quantitative studies.

**Table 3.**  $\text{SO}_2$  binding (%) in cinder and different chemisorption solutions.

Content of CaO, wt. %	$\text{SO}_2$		$\text{SO}_2$		$\text{SO}_2$	
	Cinder, 30 wt. % of Sulfidation Agent	$\text{H}_2\text{O}_2$	Cinder, 30 wt. % of Sulfidation Agent	$\text{Na}_2\text{CO}_3$	Cinder, 30 wt. % of Sulfidation Agent	$\text{Ca}(\text{OH})_2$
3	39.0	61.0	30.9	69.1	39.1	60.9
6	57.8	42.2	68.1	31.9	46.5	53.5
9	66.5	33.5	65.1	34.9	48.3	51.7

The addition of calcium oxide reduced the sulfur dioxide content in the flue gases by binding it to the non-volatile compound  $\text{CaSO}_4$ . In addition, sulfur dioxide interacted with calcium carbonate (a mineral within the sulfide ore). However, at 30 wt. pct sulfidation ore content, the degree of absorption was incomplete for all CaO amounts (Table 3). For this reason, sulfidation roasting was further carried out using lower contents (10 wt. pct and 20 wt. pct) of the pyrite-bearing ore. At these contents, the almost complete sulfidation of Pb and Zn compounds was observed according to the XRD data (Figures 4 and 5).

The  $\text{Ca}(\text{OH})_2$  suspension was used as a sulfur dioxide absorber for the flue gases of the investigated roasting process, using a content of the sulfidation agent at 10–20 wt. pct, and the CaO additive—6 wt. pct. The roasting time was 30 min at a temperature of 650 °C. According to the XRD analysis of the cinder (Figure 7a,b), the final lead- and zinc-containing compounds were galena ( $\text{PbS}$ ) and sphalerite ( $\text{ZnS}$ ). It was also found that the addition of CaO led to a significant increase in the anhydrite  $\text{CaSO}_4$  content up to 19.13–27.30 pct (while roasting without the addition resulted in a CaO content of only 3.8–5.9 pct).

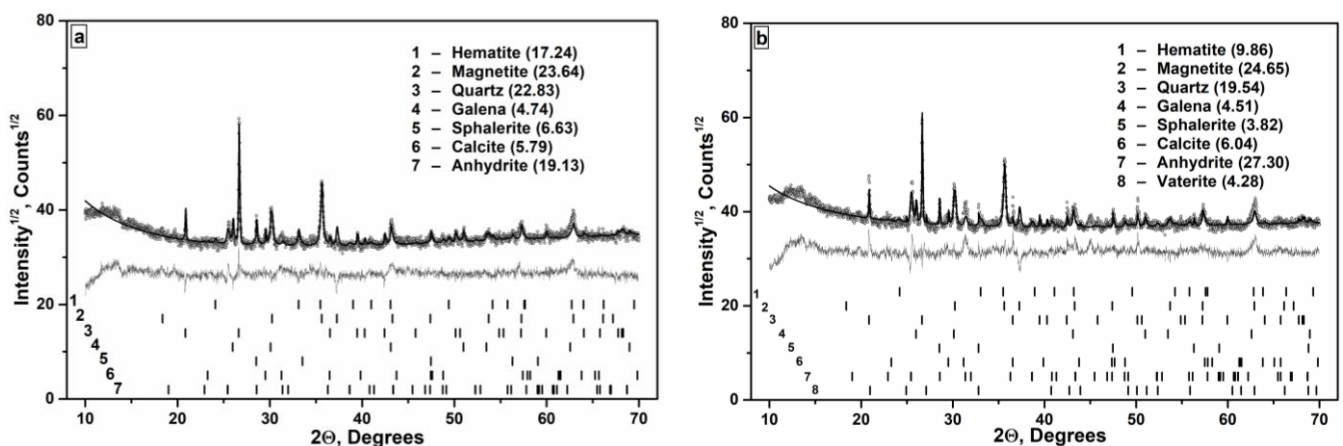


**Figure 7.** XRD of the samples cinders with the addition of 6 wt. pct CaO: (a) at 10 wt. pct sulfidation agent; (b) at 20 wt. pct sulfidation agent.

It was experimentally established that sulfur dioxide was formed from the very beginning of the process and reacted with calcium oxide in the cinder during the first ten minutes of roasting. According to the XRD data (Figure 8), the main compounds of the evaporated sludge in the absorber were portlandite  $\text{Ca}(\text{OH})_2$  (85.05 wt. pct), hannebachite  $(\text{CaSO}_3 \cdot 0.5\text{H}_2\text{O})$  (9.16 wt. pct), and calcite  $(\text{CaCO}_3)$  (5.78 wt. pct). Thus, the degree of the  $\text{SO}_2$  binding rate in the cinder was 92.13 pct when the oxidized ore was burned together with a pyrite-bearing ore and calcium oxide addition (20 wt. pct and 6 wt. pct, respectively).

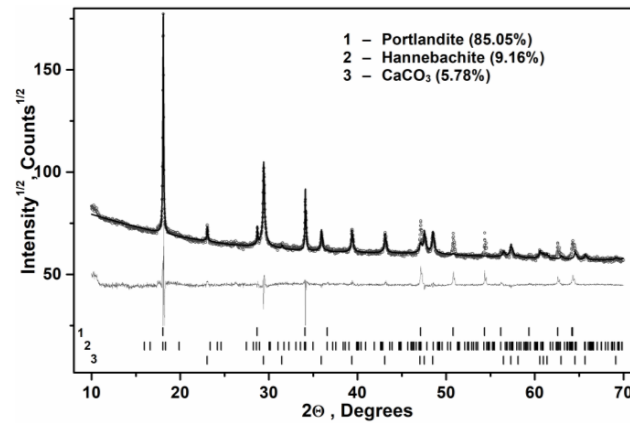


Figure 8. XRD of a sample of evaporated sludge from the absorber (20 wt.% of the sulfidation agent).

Similarly, when the 10 wt. pct sulfide ore and 6 wt. pct calcium oxide were added, the  $\text{SO}_2$  binding rate was 99.97 pct. In this case, the main compounds of the evaporated sludge in the absorber were portlandite  $(\text{Ca}(\text{OH})_2)$  (84.53 wt. pct), hannebachite  $(\text{CaSO}_3 \cdot 0.5\text{H}_2\text{O})$  (0.03 wt. pct), and calcite  $(\text{CaCO}_3)$  (15.44 wt. pct) (Figure 9), based on the material balance and XRD data.

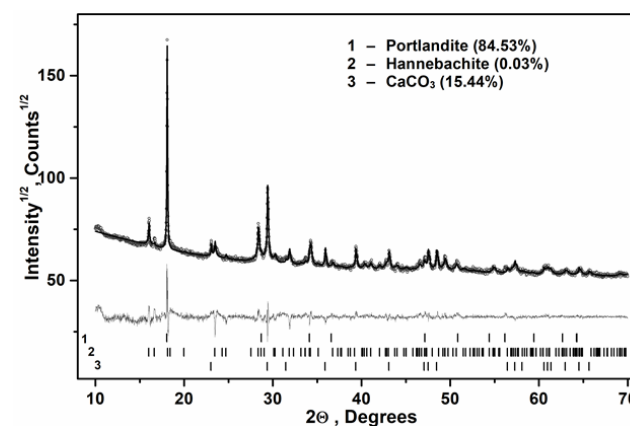


Figure 9. XRD of a sample of evaporated sludge from the absorber (10 wt. pct of the sulfidation agent).

The distribution of sulfur dioxide gas (pct) between the cinder and the absorber sludge at different sulfidation agent contents is shown in Table 4.

Table 4.  $\text{SO}_2$  binding in the cinder and in the  $\text{Ca}(\text{OH})_2$  absorber.

Content of CaO, wt. %	30 wt.% of Sulfidation Agent		20 wt.% of Sulfidation Agent		10 wt.% of Sulfidation Agent	
	$\text{SO}_2$		$\text{SO}_2$		$\text{SO}_2$	
	Cinder	Sludge	Cinder	Sludge	Cinder	Sludge
6	46.5	53.5	92.1	7.9	99.97	0.03

The experimental conditions were also tested on a larger mass sample (60 g). The laboratory setup included a vertical tube furnace and a flue gas collection system. The following parameters were used: sulfidation agent content—14 wt. pct, CaO additive—6 wt. pct, particle size—0.25 mm, and firing time—30 min. It was demonstrated that the roasting of this mixture at 650 °C led to the formation of sphalerite (ZnS), galena (PbS), magnetite (Fe<sub>3</sub>O<sub>4</sub>), hematite (Fe<sub>2</sub>O<sub>3</sub>), and anhydrite (CaSO<sub>4</sub>); such a composition can significantly facilitate further flotation enrichment (Figure 10). The degree of SO<sub>2</sub> binding in the cinder (using sulfide ore and calcium oxide contents of 14 wt. pct and 6 wt. pct, respectively) was 98.1 pct.

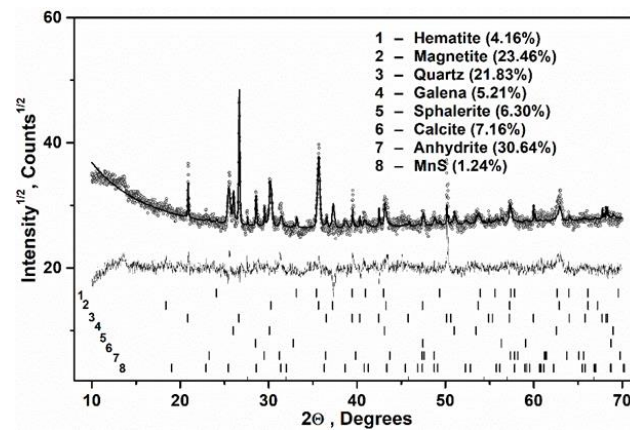


Figure 10. Rietveld refined XRD pattern of a sample of cinder.

Additional examination of the cinder using a LEO-1430VP electron microscope confirmed the presence of newly formed phases, including galena (PbS), sphalerite (ZnS), iron oxides, and anhydrite (CaSO<sub>4</sub>) (Figure 11).

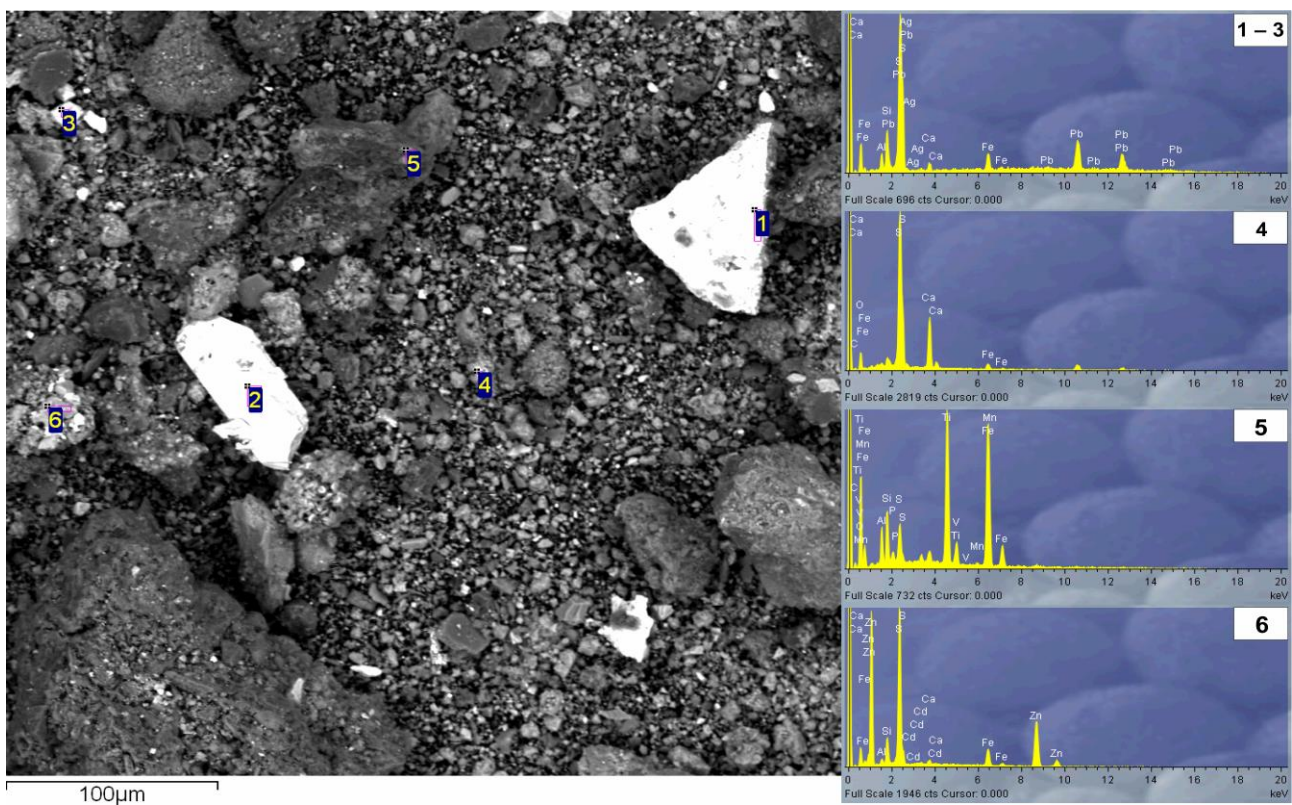


Figure 11. SEM image of the cinder: 1–3—galena grains (Gal); 4—a grain of newly formed anhydrite (Anh); 5—an aggregate of magnetite (Mag); 6—an irregularly shaped grain of sphalerite (Sph).

Thus, the process of co-roasting the oxidized ore containing plumbojarosite together with the refractory sulfide ore (characterized by the intergrowth of FeS, ZnS, and PbS crystals) was studied. It was demonstrated that the selective oxidation of pyrite was accompanied by the disintegration of intergrown crystals of PbS and ZnS, and the sulfidation of oxidized minerals. The theoretical justification for these processes was also provided. The binding of SO<sub>2</sub> in the cinder reached 98.1 pct at sulfide ore and calcium oxide contents of 14 wt. pct and 6 wt. pct, respectively. The potential for the nearly complete utilization of SO<sub>2</sub> in flue gases was demonstrated through the addition of calcium oxide to the initial mixture, which effectively bound SO<sub>2</sub> into a solid compound (CaSO<sub>4</sub>).

The optimum parameters for the sulfidation process were determined: roasting temperature—650 °C, duration—30 min, sulfidation ore content—10–15 wt. pct, calcium oxide content—6 wt. pct.

These conditions have been shown to be the most effective in activating complex minerals and reducing the amount of sulfur-containing flue gases. The approach described in this paper can improve production efficiency by increasing the reserves of ore that can be processed.

#### 4. Conclusions

This paper presents a novel approach to the flotation of oxidized ore containing goethite and plumbojarosite. The method involves co-roasting the oxidized ore with refractory sulfide lead–zinc ore from the same deposit (the Ozernoye deposit), with the addition of calcium oxide to the process. This method enables the activation of mineral complexes and the sulfidation of the oxidized minerals of lead and zinc. The addition of calcium oxide into the process facilitated the binding of sulfur dioxide, thereby reducing its content in the flue gases to 1–2 pct. Additionally, a portion of the sulfur dioxide was bound by calcium carbonate, which is a component of the sulfide ore. It has been demonstrated that roasting the ore at 650–700 °C results in the formation of new minerals, including sphalerite (ZnS), galena (PbS), magnetite (Fe<sub>3</sub>O<sub>4</sub>), hematite (Fe<sub>2</sub>O<sub>3</sub>), and anhydrite (CaSO<sub>4</sub>). However, galena and sphalerite, which are components of the original sulfide ore, did not undergo any changes during this process. Due to its composition, this roasted product can serve as a lead–zinc raw material suitable for flotation enrichment.

**Author Contributions:** I.G.A.: Conceptualization, Writing—original draft, Supervision, Project administration; P.A.G.: Data curation, Investigation, Visualization; A.D.B.: Methodology, Data curation, Validation, Formal analysis; I.P.D.: Investigation, Formal analysis; D.P.K.: Visualization, Writing—review and editing, Resources. All authors have read and agreed to the published version of the manuscript.

**Funding:** The study was carried out within the framework of the state assignment of the Baikal Institute of Nature Management, SB RAS; Project No. AAAA-A21-121011890003-4.

**Data Availability Statement:** The data presented in this study are available on request from the corresponding author.

**Acknowledgments:** The authors express their gratitude to Bulat B. Damdinov (N.L. Dobretsov Geological Institute SB RAS, Russia) for his kind assistance in the mineragraphic studies. The research was conducted using the resources of the Research Equipment Sharing Center of BINM SB RAS (Ulan-Ude, Russia).

**Conflicts of Interest:** The authors declare that there are no conflicts of interest. The authors alone are responsible for the content and writing of the article. The funders had no role in the design of the study in the collection, analyses, or interpretation of data; in the writing of the manuscript; or in the decision to publish the results.

#### References

1. Migachev, I.F.; Karpenko, I.A.; Petrash, N.G.; Karpukhina, M.V.; Kulikov, D.A.; Cheremisin, A.A. Optimal use of the mineral resource base of lead and zinc deposits in the Republic of Buryatia. *Ores Met.* **2008**, *2*, 7–19.

2. Dugarzhapova, D.B. Mineral resources sector in the economy of the Republic of Buryatia: Current state and trends. *BSU Bull. Econ. Manag.* **2021**, *4*, 42–51. [[CrossRef](#)]
3. Bakhtin, V.I.; Yalovik, G.A. State and prospects for the development of the mineral resource base of the Republic of Buryatia until 2020. *Prospect Prot. Miner. Resour.* **2007**, *12*, 6–15.
4. Pashkevich, M.A.; Petrova, T.A. Technogenic impact of sulphide-containing wastes produced by ore mining and processing at the Ozernoe deposit: Investigation and forecast. *J. Ecol. Eng.* **2017**, *18*, 127–133. [[CrossRef](#)] [[PubMed](#)]
5. Nefed'ev, M.A. *Volumetric Model and Assessment of the Prospects of the Ozerninsky Ore Cluster Based on Geophysical Data (Western Transbaikalia)*; Publishing House BSC SB RAS: Ulan-Ude, Russia, 2009; pp. 146–158.
6. Gordienko, I.V. Strategic minerals resources of the Republic of Buryatia: Current state and development prospects. *Earth Sci. Subsoil Use* **2020**, *43*, 8–35. [[CrossRef](#)]
7. Distanov, E.G.; Kovalev, K.R. *Textures and Structures of Hydrothermal-Sedimentary Pyrite-Polymetallic Ores of the Ozernoe Deposit*; Science: Novosibirsk, Russia, 1975; pp. 37–48.
8. Kovalev, K.R.; Buslenko, A.I. *Hydrothermal-Sedimentary Ore Genesis and Polymetamorphism of Ores of the Ozerninsky Ore Cluster (Western Transbaikalia)*; Science: Novosibirsk, Russia, 1992; pp. 11–34.
9. Gordienko, I.V.; Nefed'ev, M.A. The Kurba-Eravna ore district of Western Transbaikalia: Geological and geophysical structure, types of ore deposits, predictive assessment, and mineral-resource potential. *Geol. Ore Depos.* **2015**, *57*, 101–110. [[CrossRef](#)]
10. Nayak, A.; Jena, M.S.; Mandre, N.R. Beneficiation of Lead-Zinc Ores—A Review. *Miner. Process. Extr. Metall. Rev.* **2022**, *43*, 564–583. [[CrossRef](#)]
11. Klimenko, N.G.; Akhmedov, A.Z. Ways of effective use of oxidized polymetallic ores. *Ores Met.* **1996**, *6*, 66–69.
12. Caproni, G.; Ciccu, R.; Trudu, I. Processing of Oxidized and Mixed Oxide-Sulfide Lead-Zinc Ores. In *Processing of the 13th International Minerals Congress, Warsaw, Poland, 4–9 June 1979*; Elsevier Scientific: Amsterdam, The Netherlands, 1979.
13. Wet, J.R.; Singleton, J.D. Development of a viable process for the recovery of zinc from oxide ores. *J. S. Afr. Inst. Min. Metall.* **2008**, *108*, 253–259.
14. Luo, L.; Zhang, X.; Wang, H.; Zheng, B.; Wie, C. Comparing strategies for iron enrichment from Zn- and Pb-bearing refractory iron ore using reduction roasting-magnetic separation. *Powder Technol.* **2021**, *393*, 333–341. [[CrossRef](#)]
15. Mütelloğlu, N.A.; Yekeler, M. Beneficiation of Oxidized Lead-Zinc Ores by Flotation Using Different Chemicals and Test Conditions. *J. Min. Sci.* **2019**, *55*, 327–332. [[CrossRef](#)]
16. Hoerber, L.; Steinlechner, S. A comprehensive review of processing strategies for iron precipitation residues from zinc hydrometallurgy. *Clean. Eng. Technol.* **2021**, *4*, 100214. [[CrossRef](#)]
17. Lan, Z.; Lai, Z.; Zheng, Y.; Lv, J.; Pang, J.; Ning, J. Recovery of Zn, Pb, Fe and Si from a low-grade mining ore by sulfidation roasting-beneficiation-leaching processes. *J. Cent. South Univ.* **2020**, *27*, 37–51. [[CrossRef](#)]
18. Min, X.; Jiang, G.; Wang, Y.; Zhou, B.; Xue, K.; Ke, Y.; Xu, Q.; Wang, J.; Ren, H. Sulfidation roasting of zinc leaching residue with pyrite for recovery of zinc and iron. *J. Cent. South Univ.* **2020**, *27*, 1186–1196. [[CrossRef](#)]
19. Zheng, Y.; Liu, W.; Qin, W.; Jiao, F.; Han, J.; Yang, K.; Luo, H. Sulfidation roasting of lead and zinc carbonate with sulphur by temperature gradient method. *J. Cent. South Univ.* **2015**, *22*, 1635–1642. [[CrossRef](#)]
20. Li, Y.; Wang, J.; Wei, C.; Liu, C.; Ji-Bo Jiang, J.; Wang, F. Sulfidation roasting of low grade lead-zinc oxide ore with elemental sulfur. *Miner. Eng.* **2010**, *23*, 563–566. [[CrossRef](#)]
21. Han, J.; Liu, W.; Zhang, T.; Xue, K.; Li, W.; Jiao, F.; Qin, W. Mechanism study on the sulfidation of ZnO with sulfur and iron oxide at high temperature. *Sci. Rep.* **2017**, *7*, 42536. [[CrossRef](#)]
22. Zeng, P.; Wang, C.; Li, M.; Wei, C.; Ma, B.; Li, X.; Deng, Z.; Wie, X. Volatilization behavior of lead, zinc and sulfur from flotation products of low-grade Pb-Zn oxide ore by carbothermic reduction. *Powder Technol.* **2024**, *433*, 119185. [[CrossRef](#)]
23. Desogus, P.; Manca, P.P.; Orrù, G. Heavy metal leaching of contaminated soils from a metallurgical plant. *Int. J. Min. Reclam. Environ.* **2012**, *27*, 202–214. [[CrossRef](#)]
24. Zhang, B.; Guo, X.; Wang, Q.; Tian, Q. Thermodynamic analysis and process optimization of zinc and lead recovery from copper smelting slag with chlorination roasting. *Trans. Nonferr. Met. Soc. China* **2021**, *31*, 3905–3917. [[CrossRef](#)]
25. Hajati, A.; Soltani, F. Concentrating challenges of the Zarigan complex Pb-Zn-Fe non-sulfide ore: Défis de concentration du minerai complexe non sulfuré Pb-Zn-Fe de Zarigan. *Can. Metall. Q.* **2022**, *62*, 301–310. [[CrossRef](#)]
26. Mweene, L.; Gomez-Flores, A.; Jeong, H.E.; Ilyas, S.; Kim, H. Challenges and Future in Ni Laterite Ore Enrichment: A Critical Review. *Miner. Process. Extr. Metall. Rev.* **2023**, *45*, 539–563. [[CrossRef](#)]
27. Wani, O.B.; Khan, S.; Shoaib, M.; Gonçalves, C.C.; Chen, Z.; Zeng, H.; Bobicki, E.R. Processing of low-grade ultramafic nickel ores: A critical review. *Miner. Eng.* **2024**, *218*, 108976. [[CrossRef](#)]
28. Antropova, I.G.; Dambaeva, A.Y.; Danzheeva, T.Z. Sulfidizing steam roasting application in oxidized plumbiferous ores processing circuits. *Obogashchenie Rud.* **2016**, *6*, 3–8. [[CrossRef](#)]
29. Antropova, I.G.; Dambaeva, A.Y. Sulfidation of rebellious oxidized lead and zinc minerals in aqueous vapor environment. *J. Min. Sci.* **2015**, *51*, 174–178. [[CrossRef](#)]
30. Antropova, I.G.; Merinov, A.A.; Gulyashinov, P.A.; Damdinov, D.D. Sulfidation of Oxidized Lead and Zink with Pyrite-Bearing Lead-and-Zink Ore. *J. Min. Sci.* **2023**, *59*, 465–474. [[CrossRef](#)]
31. Zhang, H.; Yu, H.; Sun, W.; Lin, S.; Zhang, C. Beneficiation of silver and silver-bearing lead-zinc ores: A review. *Miner. Eng.* **2024**, *208*, 108608. [[CrossRef](#)]

32. Lopez, R.; Jordao, H.; Hartmann, R.; Ammala, A.; Carvalho, M. Study of butyl-amine nanocrystal cellulose in the flotation of complex sulphide ores. *Colloids Surf. A Physicochem. Eng. Asp.* **2019**, *579*, 123655. [[CrossRef](#)]
33. Omarova, N.K.; Sherembaeva, R.T.; Imashev, A.Z. Flotation of sulfide lead-zinc ores of the Akzhal deposit. *Obogashchenie Rud.* **2022**, *2*, 25–28. [[CrossRef](#)]
34. Algebraistova, N.K.; Prokopiev, I.V.; Komarova, E.S. Preparation of collective lead-zinc concentrates for selection cycle. *Tsvetnye Met.* **2021**, *4*, 12–17. [[CrossRef](#)]
35. Lorenzo-Tallafigo, J.; Iglesias-González, N.; Mazuelos, A.; Romero, R.; Carranza, F. An alternative approach to recover lead, silver and gold from black gossan (polymetallic ore), Study of biological oxidation and lead recovery stages. *J. Clean. Prod.* **2019**, *207*, 510–521. [[CrossRef](#)]
36. Zhang, P.; Ou, L.; Zeng, L.; Zhou, W.; Fu, H. MLA-based sphalerite flotation optimization: Two-stage roughing. *Powder Technol.* **2019**, *343*, 586–594. [[CrossRef](#)]
37. Aleksandrova, T.N.; Heide, G.; Afanasova, A.V. Assessment of refractory gold-bearing ores based of interpretation of thermal analysis data. *J. Min. Inst.* **2019**, *235*, 30–37. [[CrossRef](#)]
38. Dong, Z.; Zhu, Y.; Han, Y.; Gu, X.; Jiang, K. Study of pyrite oxidation with chlorine dioxide under mild conditions. *Miner. Eng.* **2019**, *133*, 106–114. [[CrossRef](#)]
39. Masdarian, M.; Azizi, A.; Bahri, Z. Mechanochemical sulfidization of a mixed oxide-sulphide copper ore by co-grinding with sulfur and its effect on the flotation efficiency. *Chin. J. Chem. Eng.* **2020**, *28*, 743–748. [[CrossRef](#)]
40. Fedotov, P.K.; Senchenko, A.E.; Fedotov, K.V.; Burdonov, A.E. Studies of enrichment of sulfide and oxidized ores of gold deposits of the Aldan shield. *J. Min. Inst.* **2020**, *242*, 218–227. [[CrossRef](#)]
41. Biondi, J.C.; Borgo, A.; Chauvet, A.; Monie, P.; Bruguier, O.; Ocampo, R. Structural, mineralogical, geochemical and geochronological constraints on ore genesis of the gold-only Tocantinzinho deposit (Para State, Brazil). *Ore Geol. Rev.* **2018**, *102*, 154–194. [[CrossRef](#)]
42. Myazin, V.P.; Litvintseva, V.I. Mining prospect of new selective reagents to improve the efficiency of lead-zinc ores flotation of Novo-shirokinsk deposit. *Bull. Transbaikal Univ.* **2017**, *23*, 4–15. [[CrossRef](#)]
43. Morachevsky, A.S. *Thermodynamic Calculations in Metallurgy*; Metallurgy: Moscow, Russia, 1985; p. 208.
44. Ravdelya, A.A.; Ponomareva, A.M. *Brief Reference Book of Physical and Chemical Quantities: Handbook*; Chemical Rubber Publishing Co.: Leningrad, Russia, 1983; p. 231.
45. Krestovnikov, A.N.; Vladimirov, L.P.; Gulyanitsky, B.S.; Fisher, A.Y. *Handbook for Calculations of Equilibria of Metallurgical Reactions*; Metallurgizdat: Moscow, Russia, 1963; p. 316.
46. Rahmani, F.; Mowla, D.; Karimi, G.; Golkar, A.; Rahmatmand, B. SO<sub>2</sub> removal from simulated flue gas using various aqueous solutions: Absorption equilibria and operational data in a packed column. *Sep. Purif. Technol.* **2015**, *153*, 162–169. [[CrossRef](#)]
47. Han, J.W.; Hassoli, N.; Lee, K.S.; Park, S.S.; Kim, K.D.; Kim, H.T.; Park, Y.O. Dry scrubbing of gaseous HCl and SO<sub>2</sub> with hydrated lime in entrained mixing reactor. *Powder Technol.* **2021**, *393*, 471–481. [[CrossRef](#)]
48. Dubinin, Y.; Zavarukhin, S.; Simonov, D.; Yazykov, N.; Yakovlev, V. Absorption of SO<sub>2</sub> in Fixed-bed Calc. *Katal. V. Promyshlennosti* **2015**, *15*, 6–10. [[CrossRef](#)]
49. Nechaeva, M.V. Analysis of methods for cleaning flue gases from sulfur dioxide during thermal disposal of drill cuttings. *MSoE* **2016**, *4*, 142–147.
50. Nie, Y.; Dai, J.; Hou, Y.; Zhu, Y.; Wang, C.; He, D.; Mei, Y. An efficient and environmentally friendly process for the reduction of SO<sub>2</sub> by using waste phosphate mine tailings as adsorbent. *J. Hazard. Mater.* **2020**, *388*, 121748. [[CrossRef](#)] [[PubMed](#)]

**Disclaimer/Publisher's Note:** The statements, opinions and data contained in all publications are solely those of the individual author(s) and contributor(s) and not of MDPI and/or the editor(s). MDPI and/or the editor(s) disclaim responsibility for any injury to people or property resulting from any ideas, methods, instructions or products referred to in the content.